2022 7th IEEE International Conference on Data Science in Cyberspace (DSC) | 978-1-6654-7480-1/22/$31.00 ©2022 IEEE | DOI: 10.1109/DSC55868.2022.00085

Classification of Diabetic Retinopathy Based on B-ResNet

Zhang Ying
School of Computer (National Demonstrative Software School), Beijing University of Posts and Telecommunications, Beijing, China
Key Laboratory of Trustworthy Distributed Computing and Service (BUPT), Ministry of Education
Beijing, China
email:bxzy1998@bupt.edu.cn

***Abstract*—Diabetic retinopathy is a common, difficult to diagnose and high-risk blinding disease, which requires a high professional level of doctors. However, there is a problem of uneven distribution of medical resources in China, so the construction of an automatic classification instrument for diabetic retinopathy has important research value. Methods: Eye-PACS, MESSIDOR-2 and IDRiD data sets were used to construct the data set of diabetic retinopathy by image cleaning, amplification and normalization. Meanwhile, the improved image preprocessing method was used to enhance the features of fundus images. Combining the advantages of ResNet50 feature extraction and BCNN feature fusion, the B-ResNet model was constructed. In addition, before feature fusion, the feature images extracted by ResNet50 were processed by channel attention module. At the same time, ImageNet was used to pre-train ResNet50's residual structure and fine-tune its parameters through transfer learning. Results: The accuracy of B-ResNet model reached 71.11%, ACA reached 0.714, Kappa reached 0.634 and macro-F1 reached 0.711, which were higher than previous work. And the comparison experiment proved that the improved image processing method improved the accuracy, ACA, Kappa and macro-F1 value of the model.**

Keywords—Image Processing, Diabetic Retinopathy, Deep Learning, Residual Network, Transfer Learning

I. INTRODUCTION

Diabetes is one of the three major chronic diseases in the world, which does great harm to human health. According to statistics, the number of diabetes patients in China has reached 130 million by 2020, and diabetes has become the second major chronic disease in China [1,2]. The most common complication of diabetes is retinopathy. Diabetic retinopathy (DR) is irreversible and is highly likely to cause blindness if not treated promptly [3,4,5]. Therefore, early screening and diagnosis of diabetes are of great significance. At present, doctors mainly diagnose DR grade based on fundus images, which has high requirements for doctors' professional level. However, there is a problem of uneven distribution of medical resources in China[6,7], which cannot meet the needs of the huge domestic DR patient group. Therefore, intelligent diagnosis of DR is of great research value.

In recent years, convolutional neural networks have achieved remarkable results in the field of image classification, especially the ResNet[8], which solved the degradation problem of deep networks. However, due to the small and scattered lesions, it is difficult to directly apply these excellent convolutional neural networks to DR classification. Therefore, many researchers are studying how to better apply convolutional neural network in the field of DR classification. Gargeya [9] proposed intelligent diagnosis of DR based on ResNet model, extracted 1024 features learned by the model from the last global average pooling layer, constructed a visual thermal map, and trained a tree binary classification model to classify DR images and health images; Pratt [10] used CNN model to complete DR classification. Sun Yuchen [11] proposed that DetectionNet could complete the DR classification task. Ting [12] proposed a VGG19-based deep learning system, which collected 10 sets of data from 6 different countries to verify the model and tested it in the Singapore Comprehensive DR detection project for 5 years. Bajwa[13] proposed feature fusion based on five models and carried out 2, 3 and 4 classification of DR images respectively. Experimental results proved that when there were more categories in the classification task, the classification result after feature fusion would be better than that of a single network. Gulshan [14] used InceptionV3 network to complete DR classification. Li [15] used transfer learning to detect the existence of DR, fine-tuned the pre-trained CNN model for feature extraction of fundus images, and realized classification through feature extraction training SVM. Wan Shaohua and Liang Yan [16] introduced convolutional neural network into DR detection and analyzed the effects of AlexNet, VGGNet, GoogLeNet and ResNet models in DR grade classification. Wang[17] designed a hierarchical multi-task deep learning framework to classify the grade of DR and related lesions. Salvi [18] used transfer learning to perform predictive analysis on DR. Gu Tingfei [19] proposed a method combining multi-channel attention for DR grade classification.

Through the above investigation, it was found that the fine-grained properties of the image was ignored in the DR classification method. DR classification is based on the type and number of fundus lesions, and these lesions are often scattered. Therefore, to improve network efficiency, this paper has made improvements from the following two aspects:

- The image preprocessing method has been improved to make the features of fundus lesions more obvious, so as to help the network model learn the image features and improve the classification accuracy.
- This paper has proposed B-ResNet, which integrates ResNet and fine-grained image classification method

DOI 10.1109/DSC55868.2022.00085

BCNN[20]. The ResNet enables deep network to learn more image features, and the BCNN can fuse model features. Meanwhile, before feature fusion, B-ResNet has added channel attention module to improve classification accuracy.

II. METHOD

A. Data Sets

The International Association of Ophthalmology divides DR into five grades, corresponding to 0, 1, 2, 3 and 4 labels respectively. The types and number of lesions produced by DR at different lesion stages are different, which can be roughly divided into microaneurysms, hemorrhages, hard exudates, soft exudates and hyperplasia of blood vessels. The morphological characteristics of different lesions are shown in Fig. 1. Different lesion characteristics of DR in different periods are used to diagnose DR grade, and DR grade standards are shown in TABLE I. It can be seen from TABLE I that pathological manifestations of different degrees have their own characteristics but are correlated with each other, and the change of DR grade is the result of the gradual deterioration of the disease.

Eye-PACS [21], MESSIDOR-2 [22] and IDRiD[23] were used in this paper. Eye-PACS's fundus images are provided by several hospitals and contain tens of thousands of high-resolution color fundus images taken under various conditions. The advantage of this data set is the large amount of data. It covers 5 levels of DR images, but there are serious problems such as uneven data distribution and poor image quality. Fundus images from MESSIDOR-2 are provided by three different ophthalmological institutions with good image quality, but it has less data and lacks level 4 DR images. The fundus images in IDRiD are provided by an eye clinic in India, and the image quality is good, covering 5 levels of DR images. The distribution among data classes is basically uniform, but the data volume is too small.

B. Data Preprocessing

Firstly, the data was cleaned to eliminate the interference caused by factors such as light. The black background area of the image was removed by clipping to highlight the effective features.

Secondly, through analysis, it is found that the sample image had serious inter-class imbalance, so the data was expanded by means of random rotation and flipping of images. And the image size was converted to 256×256. The data cleaning and expansion results are shown in TABLE II.

Then, feature enhancement was performed on the image. This paper used the preprocessing method of [24], as shown in (1).

$$I(x,y;\sigma)=4\big(I(x,y)-G(x,y;\sigma)*I(x,y)\big)+128 \quad (1)$$

Where $I(x,y)$ is the input image, $I(x,y;\sigma)$ is the output image, $G(x,y;\sigma)$ is a Gaussian smoothing function. σ is a parameter of the Gaussian function that evaluates the background of an image to improve contrast. Using a gaussian kernel of size (0,0), the standard deviation in both X and Y directions is 4.

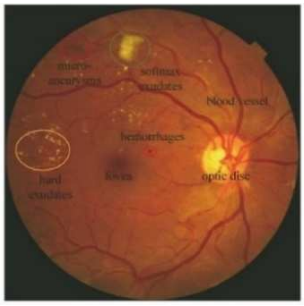

Fig. 1. Example of 2D color fundus image

TABLE I. DR CLASSIFICATION STANDARD

Category Label	Medical Interpretation	
	Retinopathy grade	*Clinical manifestation*
0	No lesions	No pathological features
1	Mild nonproliferative lesions	Microaneurysms and small hemorrhages were present
2	Moderate nonproliferative lesions	Yellow and white hard exudates and hemorrhages appeared
3	Severe nonproliferative lesions	White batting spots and bleeding spots
4	Proliferative lesion	Proliferation of blood vessels

TABLE II. DATA DISTRIBUTION

Data Sets	The Number of Images Per Category				
	Lable 0	*Lable 1*	*Lable 2*	*Lable 3*	*Lable 4*
MESSIDOR-2	547	153	246	254	-
Eye-PACS	25810	2443	5292	873	708
IDRiD	168	25	168	93	62
Clean&Enhanced & extraction	1550	1321	1568	1035	1030

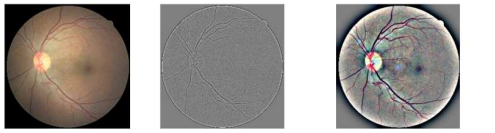

(a)Original Image (b) Processed in [24] (c) Processed in this paper

Fig. 2. Image comparison before and after processing

According to the experiment, if the image was saved in BGR format before image processing using (1), the feature enhancement effect will be more obvious, as shown in Fig. 2.

Finally, the image was normalized. Dividing each pixel value of the image by 255 to normalize the interval [0,1]. Then, calculating the mean and variance of the three channels of the image respectively, and approximating the distribution of the pixel value of the image to gaussian distribution through the zero-centered.

C. B-ResNet

Since the fundus lesions are small and scattered, B-ResNet used the channel attention module and feature fusion to process the features learned by ResNet. ResNet was known to enable deeper learning of networks, and BCNN's bilinear feature fusion can improve the accuracy of fine-grained image classification.

In this paper, the deep image information learned by ResNet was fused. And in order to highlight the location and number of lesions in the fusion process, the channel attention module was used to process the features learned by ResNet and feature fusion was carried out after ReLU. The B-ResNet model structure is shown in Fig. 4.

1) Residual Model: ResNet50 was selected in this paper as the baseline model [25], which added residual unit through short-circuit mechanism on the basis of VGGNet stack [26]. That is, when the features learned by input x were denoted as H(x), the learned residual was H(x)-x. The residual element used in this paper is shown in Fig. 3. The residual unit shown in Fig. 3 was adapted to a deeper residual network and could learn more features, which was particularly important for fine-grained classification tasks. In addition, when the size of feature graph was reduced by half, the number of feature graph was doubled, which also keeped the complexity of network layer.

2) Channel Attention Module: To make the model focus on the more "important" channels, the weight of each channel was calculated and assigned to the corresponding channel before feature fusion. This paper referenced the channel attention module in CBAM[27], as shown in Fig. 5. Firstly, Average Pooling and Max Pooling were used to compress and transform feature maps into one-dimensional in spatial dimension. Then they were input into the shared MLP to obtain the weight of feature map on each channel. Since both Average Pooling and Max Pooling were used to calculate the weight of each channel, element-by-element summation was adopted to merge to generate the final channel attention diagram.

3) Bilinear Models: B-ResNet model consisted of four elements, as can be seen from (2).

$$B=(f_A, f_B, P, C) \tag{2}$$

Where, f_A and f_B represent feature extractor functions. In this paper, ResNet50 model was used as feature extractor. In order to retain enough features for fusion, the classification layer and pooling layer of ResNet50 were removed, and the feature graph learned by the last residual module was extracted. P represents the pooling function, and C is the classification function. After feature extraction device, the two characteristic matrix $f_A(l, L) \in R^{T\times M}$ and $f_B(l, L) \in R^{T\times M}$ calculated as the following:

$$b=(l, L, f_A, f_B)=f_A^T(l, L)f_B(l, L) \quad \in R^{T\times M}, \tag{3}$$

$$\xi(L)=\sum_{l}^{A} b(l, L, f_A, f_B) \quad \in R^{T\times M}, \tag{4}$$

$$x=\mathrm{vec}(\xi(L)) \quad \in R^{MN\times 1}, \tag{5}$$

$$y=\mathrm{sign}(x)\sqrt{|x|} \quad \in R^{MN\times 1}, \tag{6}$$

$$z=y/\|y\|_2 \quad \in R^{MN\times 1}, \tag{7}$$

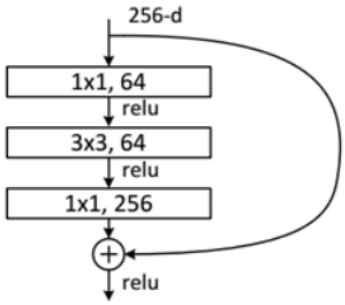

Fig. 3. Model Residual unit module

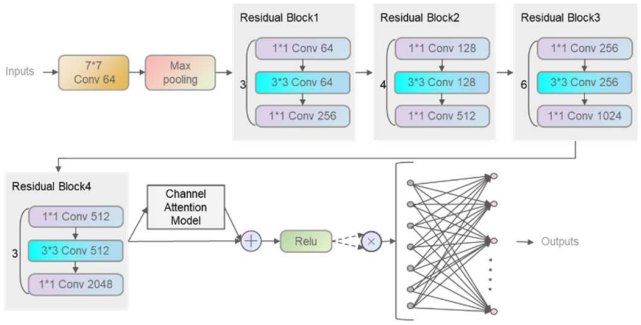

Fig. 4. B-ResNet Model

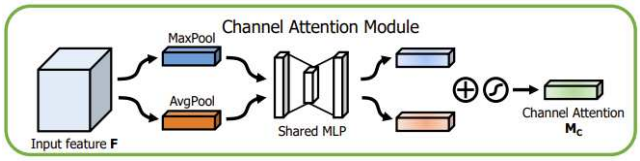

Fig. 5. Channel Attention Module

Where, b represents the result of the cross product of the feature matrix. The matrix ξ is obtained by sum pooling for b, and then transform it to vector x. Using (6) to calculate x to obtain matrix y, and then it is regularized to obtain z. Finally, feature z was converted into a one-dimensional array and sent to the fully connected network as input.

III. Result

The experimental environment of this paper was Ubuntu18.04 operating system, server CPU was Intel(R) Xeon(R) CPU E5-1660 V4.@3.20ghz, graphics card GPU was Tesla P100-DGXS, running memory was 16GB, programming environment was Python. The deep learning framework was Pytorch.

In this paper, stochastic gradient descent (Nesterov SGD) [28] was used as the optimization algorithm of the model, and dynamic learning rate was used. The initial learning rate was 0.0001 and the dynamic gradient Gamma was 0.1. A total of 1200 epochs were trained, and the learning rate changed with the 250th epoch. Meanwhile, the cross entropy loss function was used for iteration, batch size was set to 32. Initialize the residual

model with parameters pretrained with ImageNet. 70% of 6504 fundus images were used as training sets for parameter training of neural network model, 30% of them were used as a test set to verify the model training results.

According to the experimental result, the accuracy of B-ResNet reached 71.11%. The accuracy of the model in the test set and the error curve in the training set are shown in Fig. 6.

A. Evaluation Indicator

Accuracy, ACA, Kappa and macro-F1 were adopted as evaluation indexes of the algorithm in this paper.

- **Accuracy** refers to the ratio of the number of correctly classified samples to the number of samples in the test data set, and the calculation formula is shown in (8).

$$\text{Accuracy}=\frac{R_{TP}+R_{TN}}{R_{TP}+R_{FP}+R_{FN}+R_{TN}} \tag{8}$$

Where $R_{TP}+R_{TN}$ represents the number of correct predictions, And the $R_{TP}+R_{FP}+R_{FN}+R_{TN}$ represents the total number of samples.

- **ACA** is the mean of classification accuracy, which is used to measure the average level of classification accuracy. The calculation formula is shown in (9).

$$\text{ACA}=\frac{\sum_{i=1}^{n}\text{Precision}_i}{n} \tag{9}$$

Where n represents the classification category, and Precision_i represents the accuracy of class i.

- **Kappa** is used for consistency verification and can also be used to measure classification precision. Generally, Kappa falls between 0 and 1. The larger Kappa value is, the stronger the consistency of classification results is and the higher the precision is. The calculation formula is shown in (10).

$$\text{Kappa}=\frac{p_0-p_e}{1-p_e} \tag{10}$$

Where, p_0 is the sum of the correctly classified samples for each category divided by the total number of samples. Assuming that the true samples for each category are $a_1,a_2,a_3,\ldots,a_n$, and the predicted sample numbers of each category are $b_1,b_2,b_3,\ldots,b_n$, the total number of samples is n, then p_e is calculated as shown in (11).

$$p_e=\frac{a_1\times b_1+a_2\times b_2+\ldots+a_n\times b_n}{n\times n} \tag{11}$$

- **macro-F1** takes into account both accuracy and recall, and its calculation formula is shown in (12).

$$\text{macro-F1}=\frac{2}{n}\times\frac{\sum_{i=1}^{n}\text{Precision}_i\times\sum_{i=1}^{n}\text{Recall}_i}{\sum_{i=1}^{n}\text{Precision}_i+\sum_{i=1}^{n}\text{Recall}_i} \tag{12}$$

Where n represents the classification category, Precision_i represents the accuracy of class i, and Recall_i represents the recall of class i.

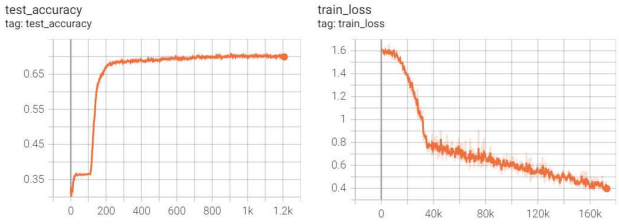

Fig. 6. Accuracy and error curve

TABLE III. COMPARISON OF EXPERIMENTAL RESULTS OF DIFFERENT NETWORKS

Model	Evaluation Indicator			
	Accuracy	*ACA*	*Kappa*	*macro-F1*
Mobilenet_V2	60.19%	0.599	0.495	0.595
Efficientnet_B4	63.37%	0.625	0.538	0.626
B-ResNet	**71.11%**	**0.714**	**0.634**	**0.711**
FGMAS	-	0.577	-	0.610
BiRA-Net	-	0.543	-	0.573
Bravo[32]	-	0.505	-	0.508
Yan Songlin[33]	65.58%	-	-	-

TABLE IV. COMPARISON OF EXPERIMENTAL RESULTS OF DIFFERENT PRETREATMENT SCHEMES

Model+ Image Processing Method	Evaluation Indicator			
	Accuracy	*ACA*	*Kappa*	*macro-F1*
B-ResNet + [24]	68.58%	0.680	0.601	0.661
B-ResNet + this paper	**71.11%**	**0.714**	**0.634**	**0.711**

B. Experimental Results

In the experiment, the proposed algorithm was not only compared with the popular convolutional neural network model Mobilenet_V2[29] and Efficientnet_B4[30], but also compared with the previous work of DR grade classification. They included FGMAS[19] and BiRA-Net[31] which are all based on feature fusion, algorithms based on CNN model Bravo[32], and algorithms based on transfer learning Yan Songlin[33]. The experimental results are shown in TABLE III. Meanwhile, this paper compared the model results by using the improved image processing method and the processing method in [24], and the experimental results are shown in TABLE IV.

IV. DISCUSSION

TABLE III shows that B-ResNet is higher than popular convolutional neural network Mobilenet_V2 and Efficientnet_B4 in terms of accuracy, Kappa, ACA and macro-F1. Compared with previous work, it is found that B-ResNet is superior to the model proposed by Yan Songlin in accuracy, and the model proposed by Bravo in ACA and macro-F1. Moreover, B-ResNet is superior to two other classification models based on feature fusion, FGMAS and BiRA-Net, in ACA and macro-F1 indices. And TABLE IV shows that under the same experimental environment and network model, compared with the preprocessing scheme in [24], the improved image

preprocessing scheme in this paper improves the accuracy, ACA, Kappa and macro-F1. It can be seen that the improved preprocessing method in this paper is more helpful for the model to learn image features.

According to the experiments, level 1 fundus images in DR classification are the most difficult to classify. Because the lesions at the initial stage are the smallest, so it is hard to find, and that is also consistent with medical logic. In level 1 fundus image classification, the accuracy of FGMAS model was 30.1%, and that of BiRA-Net was only 18.7%, while the accuracy of B-ResNet model proposed in this paper was 54.9%, far higher than the other two models.

The model proposed in this paper has a slow convergence rate and a long training time during training, which may be related to the excessively large one-dimensional feature matrix formed after feature fusion. The subsequent improvement can try to compress the feature fusion matrix to accelerate the training speed.

V. Conclusion

In this paper, ResNet50 was selected as feature extraction model and fine-tuned by transfer learning. Secondly, the channel attention module was used to further process the feature images extracted by ResNet50. Then, BCNN's feature fusion method was used to fuse the feature graph. Finally, the fused feature map was sent to the fully connected network. According to the characteristics of large distribution deviation and small number of data sets, multiple data sets and data enhancement technology were used to expand the data set to avoid model overfitting. Meanwhile, the pretreatment method of fundus images was improved to highlight fundus lesions more.

The experimental results show that the B-ResNet model proposed in this paper can improve the accuracy of the classification of DR, and has a certain reference value for promoting the study of automatic screening system for DR.

References

[1] 何蓓蕾,何媛.糖尿病与非视网膜眼部并发症相关性的研究进展[J].国际眼科杂志,2021,21(04):623-627.

[2] 刘玉华,高玲.糖尿病视网膜病变治疗研究现状、问题与展望[J].中华眼底病杂志,2016,32(02):206-210.

[3] Markoulli M, Flanagan J, Tummanapalli S S, et al. The impact of diabetes on corneal nerve morphology and ocular surface integrity[J]. The ocular surface, 2018, 16(1): 45-57.

[4] Semeraro F, Cancarini A, Rezzola S, et al. Diabetic retinopathy: vascular and inflammatory disease[J]. Journal of diabetes research, 2015, 2015.

[5] Abdelkader H, Patel D V, McGhee C N J, et al. New therapeutic approaches in the treatment of diabetic keratopathy: a review[J]. Clinical & experimental ophthalmology, 2011, 39(3): 259-270.

[6] 金涛,魏贵磊.基层医疗机构的员工流失问题研究——以乡镇医院为例[J].中国科技信息,2021(12):112-114.

[7] 张文天,孔凡悦,王权,李慧.我国卫生资源配置公平性现状及"十四五"期间公平性预测研究[J].中国卫生事业管理,2022,39(03):161-165+207.

[8] He K, Zhang X, Ren S, et al. Deep residual learning for image recognition[C]//Proceedings of the IEEE conference on computer vision and pattern recognition. 2016: 770-778.

[9] Gargeya R, Leng T. Automated identification of diabetic retinopathy using deep learning[J]. Ophthalmology, 2017, 124(7): 962-969.

[10] Pratt H, Coenen F, Broadbent D M, et al. Convolutional neural networks for diabetic retinopathy[J]. Procedia computer science, 2016, 90: 200-205.

[11] 孙雨琛,刘宇红,张达峰,张荣芬.基于深度学习的糖尿病视网膜病变诊断方法[J].激光与光电子学进展,2020,57(24):359-366.

[12] Ting D S W, Cheung C Y L, Lim G, et al. Development and validation of a deep learning system for diabetic retinopathy and related eye diseases using retinal images from multiethnic populations with diabetes[J]. Jama, 2017, 318(22): 2211-2223.

[13] Bajwa M N, Taniguchi Y, Malik M I, et al. Combining fine-and coarse-grained classifiers for diabetic retinopathy detection[C]//Annual Conference on Medical Image Understanding and Analysis. Springer, Cham, 2019: 242-253.

[14] Gulshan V, Peng L, Coram M, et al. Development and validation of a deep learning algorithm for detection of diabetic retinopathy in retinal fundus photographs[J]. Jama, 2016, 316(22): 2402-2410.

[15] Li X, Pang T, Xiong B, et al. Convolutional neural networks based transfer learning for diabetic retinopathy fundus image classification[C]//2017 10th international congress on image and signal processing, biomedical engineering and informatics (CISP-BMEI). IEEE, 2017: 1-11.

[16] Wan S, Liang Y, Zhang Y. Deep convolutional neural networks for diabetic retinopathy detection by image classification[J]. Computers & Electrical Engineering, 2018, 72: 274-282.

[17] Wang J, Bai Y, Xia B. Simultaneous diagnosis of severity and features of diabetic retinopathy in fundus photography using deep learning[J]. IEEE Journal of Biomedical and Health Informatics, 2020, 24(12): 3397-3407.

[18] Salvi R S, Labhsetwar S R, Kolte P A, et al. Predictive Analysis of Diabetic Retinopathy with Transfer Learning[C]//2021 4th Biennial International Conference on Nascent Technologies in Engineering (ICNTE). IEEE, 2021: 1-6.

[19] 顾婷菲,郝鹏翼,白琮,柳宁.结合多通道注意力的糖尿病性视网膜病变分级[J].中国图象图形学报,2021,26(07):1726-1736.

[20] Lin T Y, RoyChowdhury A, Maji S. Bilinear cnn models for fine-grained visual recognition[C]//Proceedings of the IEEE international conference on computer vision. 2015: 1449-1457.

[21] Cuadros J, Bresnick G. EyePACS: an adaptable telemedicine system for diabetic retinopathy screening[J]. Journal of diabetes science and technology, 2009, 3(3): 509-516.

[22] Decencière, E., Zhang, X., Cazuguel, G., Lay, B., Cochener, B., Trone, C., Gain, P., Ordonez, R., Massin, P., Erginay, A., Charton, B., & Klein, J. (2014). FEEDBACK ON A PUBLICLY DISTRIBUTED IMAGE DATABASE: THE MESSIDOR DATABASE. Image Analysis & Stereology, 33(3), 231-234. doi:https://doi.org/10.5566/ias.1155

[23] Prasanna Porwal, Samiksha Pachade, Ravi Kamble, Manesh Kokare, Girish Deshmukh, Vivek Sahasrabuddhe, Fabrice Meriaudeau, April 24, 2018, "Indian Diabetic Retinopathy Image Dataset (IDRiD)", IEEE Dataport, doi: https://dx.doi.org/10.21227/H25W98.

[24] Zhou K, Gu Z, Liu W, et al. Multi-cell multi-task convolutional neural networks for diabetic retinopathy grading[C]//2018 40th Annual International Conference of the IEEE Engineering in Medicine and Biology Society (EMBC). IEEE, 2018: 2724-2727.

[25] Xie S, Girshick R, Dollár P, et al. Aggregated residual transformations for deep neural networks[C]//Proceedings of the IEEE conference on computer vision and pattern recognition. 2017: 1492-1500.

[26] Alom M Z, Hasan M, Yakopcic C, et al. Improved inception-residual convolutional neural network for object recognition[J]. Neural Computing and Applications, 2020, 32(1): 279-293.

[27] Woo S, Park J, Lee J Y, et al. Cbam: Convolutional block attention module[C]//Proceedings of the European conference on computer vision (ECCV). 2018: 3-19.

[28] 纪泽宇,张兴军,付哲,高柏松,李靖波.分布式深度学习框架下基于性能感知的 DBS-SGD 算法[J].计算机研究与发展,2019,56(11):2396-2409.

[29] Howard A G, Zhu M, Chen B, et al. Mobilenets: Efficient convolutional neural networks for mobile vision applications[J]. arXiv preprint arXiv:1704.04861, 2017.

[30] Tan M, Le Q. Efficientnet: Rethinking model scaling for convolutional neural networks[C]//International conference on machine learning. PMLR, 2019: 6105-6114.

[31] Zhao Z, Zhang K, Hao X, et al. Bira-net: Bilinear attention net for diabetic retinopathy grading[C]//2019 IEEE International Conference on Image Processing (ICIP). IEEE, 2019: 1385-1389.

[32] Bravo M A, Arbeláez P A. Automatic diabetic retinopathy classification[C]//13th International Conference on Medical Information Processing and Analysis. International Society for Optics and Photonics, 2017, 10572: 105721E.

[33] 颜嵩林,林溢星,李鹤喜,赵地,迟学斌.基于多重迁移学习的糖尿病视网膜病变检测[J].中国数字医学,2019,14(03):26-30.